

# Photonic Transformers

Mark Douvidzon (✉ [mark.douvidzon@technion.ac.il](mailto:mark.douvidzon@technion.ac.il))

Technion, Israel Institute of Technology

**Shai Maayani**

Technion, Israel Institute of Technology

**Harel Nagar**

Tel Aviv University

**Tamir Admon**

Tel Aviv University

**Vladimir Shuvayev**

Queens College of CUNY

**Lan Yang**

Washington University in St. Louis <https://orcid.org/0000-0002-9052-0450>

**Lev Deych**

Queens College of CUNY, Flushing, NY 11367, USA

**Yael Roichman**

Tel Aviv University

**Tal Carmon**

Technion

---

## Research Article

### Keywords:

**Posted Date:** August 31st, 2020

**DOI:** <https://doi.org/10.21203/rs.3.rs-56565/v1>

**License:**  This work is licensed under a Creative Commons Attribution 4.0 International License.

[Read Full License](#)

---

**Version of Record:** A version of this preprint was published at APL Photonics on July 19th, 2021. See the published version at <https://doi.org/10.1063/5.0053154>.

# Abstract

Largely-deformed<sup>1–4</sup> microcavities<sup>5</sup> support instabilities suppression<sup>6</sup> chaotic ray-dynamics<sup>7</sup>, directional-emission<sup>8–10</sup>, and momentum transfer<sup>11</sup> for nonlinear optics, but such deformations are generally possible only by fabricating discrete sets of resonators. In contrast, optical tweezers<sup>12–17</sup> permit continuous large changes<sup>18–28</sup>, such as deformations from spherical dielectrics to triangular ones<sup>25</sup>. We report on transformable micro-photonic devices that change their functionality while operating. Assisted by computerized holographic-tweezers, we gradually deform the shape and change the functionality of a droplet whispering-gallery cavity. For example, we continuously deform hexagonal cavities to rectangular ones, and demonstrate switching to directionally emitting mode-of-operation, or splitting a resonant mode to a 10-GHz separated doublet. A continuous trend of improving spatial light modulators and tweezers suggests that our method is scalable to control the shape and functionality of many individual devices. We also demonstrate optional solidification proving the feasibility of transformers-enabled applications, including in printing 3D optical-circuits and multiwavelength optical-networks.

## Introduction

Micro-machines, including optical devices, are generally susceptible to small deformations that don't transform their functionality and keep their mathematical solution only weakly perturbed. Yet, optical tweezers can control the position<sup>26</sup>, orientation<sup>19,20,23</sup>, speed<sup>18,21</sup>, and shape<sup>25</sup> of dielectrics. Furthermore, optical tweezers are significant in engineering areas such as microfluidics where tweezers are utilized in various devices such as micro-motors<sup>28</sup>, -valves<sup>22,27</sup>, and -pumps<sup>24,28</sup>. In sciences including physics, biology, and chemistry, tweezers manipulate atoms<sup>12</sup>, as well as enable studying single individual RNA<sup>13</sup>-protein<sup>15</sup>-, and DNA<sup>17</sup>-molecules and interrogating them during chemical reactions. It might be surprising, therefore, that a major photonic tool – the optical tweezers, was rarely used to control photonic devices despite the large and upon-request deformations that tweezers permit<sup>25</sup>. Instead, expansion-induced deformations by thermal or stress were typically used to support, in most cases, a limited tuning of one of the system parameters. Here we use computerized optical-tweezers to induce large deformations of an optical resonator while the cavity is "hot", meaning that light is fiber-coupled<sup>29</sup> to resonate inside. We set the cavities' curvatures upon need, and tune cavities' shapes here between stadium, rectangle-like, pentagon-like, and etc.; as well as experimentally demonstrate directional emission and eigenfrequency tuning. This work lays the groundwork to develop advanced capabilities to control the shape and functionality of photonic devices upon need, arbitrarily positioning them in the form of a 3D optical-circuit configuration, and then solidifying this circuit – when desired functionality is achieved. Below we will prove the concept of diverse functionalities enabled by the on-demand control of photonic structures; and show photonics that one can reconfigure to directionally emit or largely split a resonance, with optional solidification to the form of a durable fiber-coupled device.

## Results

**In our experiments**, we use a computer-generated hologram to allocate light upon request and apply forces to deform a photonic device made of a submerged oil-droplet. The microdroplet hosts whispering-gallery modes and function as a cavity that resonate when the droplet circumference is an integer number of optical wavelengths. We start by demonstrating solidability to a durable device, and then follow reconfigure resonators to switch their functionality. For demonstrating solidability, we first evanescently couple a liquid droplet resonator to a tapered-fiber coupler<sup>29</sup> while both are submerged in a photochemically curable medium, that we will later solidify (Method 1). We control the coupling distance between the resonator and coupler while monitoring optical transmission through the resonator via the standard fiber (Fig 1. a). When coupling performance is satisfying, we cure the photochemical medium with UV light. The solidified apparatus exhibits an optical quality factor of 730,000 and coupling efficiency near 80%, as indicated by the measured resonance linewidth and by its depth (Fig 1 d). Our device (Fig 1 e) survived several falls to the floor without any degradation in performance. Our demonstrated solidification of a spherical droplet-resonator after setting its coupling-distance parameter is a first step toward solidifying photonic circuits made of many droplets. We will now deform our droplet resonators, including while they are optically active. For that, and as one can see in figure 1, we use a 20x, 1.0 NA water emersion top-view objective to observe the droplets as well as to manipulate them with optical tweezers.

The multiple traps are controlled with a spatial light modulator (SLM) and a 532 nm continuous wave (CW) laser with a typical trapping power of 0.5 Watt. Additionally, we installed a bottom-view microscope to ease controlling the shape of the droplet as well as its position relative to the tapered-fiber coupler. An important enabler in reshaping the initially spherical droplet relates to reducing the surface tension of the droplet boundary, or in simpler words – making the droplet softer. For the purpose of reducing interfacial tension, we use two emulsifiers (Method 1), one leads to oil droplets in water, while the other boosts creation of water droplets in oil, and scan their concentrations until we observe a transition region where the emulsion is indecisive either it prefers to form oil in water or water in oil drops. Such a system is generally referred to as Winsor type III emulsion. In such systems, the surfactant forms a microemulsion in a separate phase between the oil and aqueous phases. This phase is a continuous layer containing surfactants, water, and dissolved hydrocarbons. This situation is ideal for achieving ultralow interfacial-tension values and is favorable here for tweezers-deformable droplets<sup>25</sup>. The liquids we choose here were the ones that combine high optical transmission coefficient and the high refractive-index contrast between core and cladding, in accordance with what is needed to reduce optical losses by absorption and radiation. Our approach of softening the droplet resonator, and then deforming them upon demand using the tweezers, distinguishes our deformable cavities from earlier works where liquid jets were broken into falling droplets<sup>1,2</sup> and excited by free-propagating light beams. (Method 2).

As shown in figure 2, we demonstrate our ability to deform microcavities to various shapes, while evanescently coupling light into it. Figure 2 shows the deformation of an n-heptane drop into a cigar and then to shapes having 3, 4, 5, and 6-fold symmetry. The optical quality was measured by fitting the absorption lineshape to a Lorentzian function and was about half a million. The three, four, five, and six

corner measurements were performed on the same droplet, illustrating the wide range of the system's continuous-tunability. We characterize the deformation of the resonator quantitatively using parameter  $\varepsilon = \frac{r_p - r_e}{a}$  [Fig 2], where  $r_p$  and  $r_e$  are the longest and shortest radius, and  $a$  represents the undisturbed sphere radius.

In our next measurement (Fig. 3), we continuously deform the droplet resonator while optically interrogating its resonance spectrum. (See, additional Video). As figure 3 shows, stretching the resonator split its mode as expected from the relation<sup>30</sup>  $\omega(m) = \omega_0 \left\{ -\frac{\varepsilon}{6} \left[ 1 - \frac{3m^2}{l(l+1)} \right] \right\}$ , where  $\omega_0$  is the laser frequency near 384 THz,  $l$  is the polar mode number (1000), and  $m$  is the azimuthal mode number (577).  $\varepsilon = 8\%$  deformation allowed a 10.8 GHz split between two successive azimuthal modes. Next, we deform a droplet resonator to be sharper at one of its corners by using 4-fold tweezers (Fig. 4 a, green) while monitoring the tweezers using a near-infrared camera. We continue deforming the droplet, while exciting and monitoring its circumferentially circulating resonance using the camera until directional emission appears to emerge from this corner (Fig. 4, b, d). The results of the computational simulations (Method 4) are shown in Fig. 4c – one can see the directed emission out of the resonator in qualitative agreement with our experimental results.

## Conclusion

In conclusion, previous deformation technologies were only slightly deforming resonators from a shape allowing for an exact solution. As such, one could determine the optical characteristics of a deformed system as a small correction to the characteristics of an exactly solvable situation using a perturbation approach. Such a perturbative deformation was rarely permitting changing device functionality. In contrast, we report here on non-perturbative deformations (that one cannot describe using perturbation theory) that transform resonators functionality to directionally emit or broadly tuned. Unlike standard lithography, our non-perturbative deformations transform the device's functionality upon need while operating. We have demonstrated on-demand reconfiguration of photonic microresonators through computerized holographic tweezers to transform their behaviors to control light. With spatial light modulators that have 10 million pixels nowadays (and continuously improving), and with solidification that we show, our transformable photonic is scalable to many devices in a 3D photonic circuit, while controlling the shape, orientation, and position of each component when the circuit is optically active.

## Methods

### Method 1: Solidification

For the resonator, we use silicone oil with a refractive index of  $n = 1.41$ . The surrounding cladding medium is a photochemical polymer (My Polymers Ltd., QF-133-V3) with a low refractive index ( $n=1.33$ ). We pour the polymer, while in its liquid phase, to a chamber that is made from two microscope slides that further improve rigidity. We then submerge a droplet made of silicone oil and a tapered-fiber coupler in the

liquid polymer. We use the taper to evanescently couple light into the droplet resonator (26), from a tunable 780 nm laser, while monitoring its spectral transmission via the other side of the same tapered fiber. We fine-tune the coupling efficiency through moving the tapered coupler with respect to the resonator. Once we achieve a satisfactory result, we solidify the photochemical polymer with a 365 nm UV illuminator (Vilber Lourmat, VL-6.L). While the silicon oil resonator is still liquid, it is surrounded by solid walls. We did not measure any degradation of performance over weeks of operation.

## Method 2: Materials

For the resonator, we use one droplet of n-heptane oil (CAS Number: 142-82-5, Sigma-Aldrich). For the surrounding, we use deionized water. For softening the water-oil interface, we use NaCl emulsifier in 30 mM concentration and 1 mM concentration of Dioctyl sulfosuccinate sodium salt (Aerosol OT) (CAS Number 577-11-7, Sigma-Aldrich). The concentration here is relative to 1 liter of water.

## Method 3: Making the Droplets

We prefill the chamber with the water-AOT-NaCl solution (Methods), fill a syringe with n-heptane and equipped it with a 150-micron inner diameter needle. We then apply pressure on the syringe piston to ensure a steady flow of n-heptane through the syringe needle and pulled it at a steady speed through the prefilled chamber. Depending on the pulling speed and flow velocity, and in agreement with the Plateau-Rayleigh instability, we generate droplets in the desired diameter range, spatially separated from each other. Refractive index of our droplets is 1.3855 and that of their surrounding liquid is 1.3298.

## Methods 4: Numerical Simulation

We simulate the directional emission for a deformed cavity using a two-dimensional model to avoid unnecessary numerical difficulties. We utilize a 2D FEM frequency domain simulations run on COMSOL computational platform, where we compute the field emitted by a two-dimensional resonator in the form of a semicircle adjacent to an ellipse with the semi-axes 86  $\mu\text{m}$  and 75  $\mu\text{m}$ . This shape agrees most closely with the image of the deformed droplet as determined from its micrograph. The emission was associated with a WGM excited by a fiber coupler at the frequency in the vicinity of 780 nm. We did the frequency sweep around this value to find the best coupling with the waveguide.

## References

1. Hartings, J. M., Cheung, J. L. & Chang, R. K. Temporal beating of nondegenerate azimuthal modes in nonspherical microdroplets: technique for determining the distortion amplitude. *Appl Opt* **37**, 3306–3310 (1998).
2. Lee, S.-B. *et al.* Observation of Scarred Modes in Asymmetrically Deformed Microcylinder Lasers. *Phys. Rev. Lett.* **88**, 033903 (2002).
3. Cao, H. & Wiersig, J. Dielectric microcavities: Model systems for wave chaos and non-Hermitian physics. (2015) doi:10.1103/RevModPhys.87.61.

4. Nöckel, J. U. & Stone, A. D. Ray and wave chaos in asymmetric resonant optical cavities. *Nature* **385**, 45–47 (1997).
5. Vahala, K. J. Optical microcavities. *Nature* vol. 424 839–846 (2003).
6. Bittner, S. *et al.* Suppressing spatiotemporal lasing instabilities with wave-chaotic microcavities. *Science (80-. )*. **361**, 1225–1231 (2018).
7. Gmachl, C. *et al.* High-power directional emission from microlasers with chaotic resonators. *Science (80-. )*. **280**, 1556–1564 (1998).
8. Han, Z.-F. *et al.* Controlling deformation in a high quality factor silica microsphere toward single directional emission. *Appl. Opt.* **52**, 298 (2013).
9. Shinohara, S. *et al.* Chaos-assisted emission from asymmetric resonant cavity microlasers. *Phys. Rev. A* **83**, 53837 (2011).
10. Wiersig, J. & Hentschel, M. Combining directional light output and ultralow loss in deformed microdisks. *Phys. Rev. Lett.* **100**, 033901 (2008).
11. Jiang, X. *et al.* Chaos-assisted broadband momentum transformation in optical microresonators. *Science (80-. )*. **358**, 344–347 (2017).
12. Chu, S., Bjorkholm, J. E., Ashkin, A. & Cable, A. Experimental observation of optically trapped atoms. *Phys. Rev. Lett.* **57**, 314–317 (1986).
13. Huber, R. *et al.* Isolation of a hyperthermophilic archaeum predicted by in situ RNA analysis. *Nature* **376**, 57–58 (1995).
14. Grier, D. G. A revolution in optical manipulation. *Nature* **424**, 810–816 (2003).
15. Cecconi, G., Shank, E. A., Bustamante, C. & Marqusee, S. Biochemistry: Direct observation of the three-state folding of a single protein molecule. *Science (80-. )*. **309**, 2057–2060 (2005).
16. Dholakia, K. & Čižmár, T. Shaping the future of manipulation. *Nature Photonics* vol. 5 335–342 (2011).
17. Tang, S. J. *et al.* A Tunable Optofluidic Microlaser in a Photostable Conjugated Polymer. *Adv. Mater.* **30**, 1804556 (2018).
18. He, H., Friese, M. E. J. J., Heckenberg, N. R. & Rubinsztein-Dunlop, H. Direct Observation of Transfer of Angular Momentum to Absorptive Particles from a Laser Beam with a Phase Singularity. *Phys. Rev. Lett.* **75**, 826–829 (1995).
19. Friese, M. E. J. J., Nieminen, T. A., Heckenberg, N. R. & Rubinsztein-Dunlop, H. Optical alignment and spinning of laser-trapped microscopic particles. *Nature* **394**, 348–350 (1998).
20. Berglund, N. Kramers' law: Validity, derivations and generalisations. in *Markov Processes and Related Fields* vol. 19 459–490 (2013).
21. Paterson, L. *et al.* Controlled rotation of optically trapped microscopic particles. *Science (80-. )*. **292**, 912–914 (2001).
22. Terray, A., Oakey, J. & Marr, D. W. M. Microfluidic control using colloidal devices. *Science (80-. )*. **296**, 1841–1844 (2002).

23. Galajda, P. & Ormos, P. Orientation of flat particles in optical tweezers by linearly polarized light. *Opt. Express* **11**, 446 (2003).
24. Ladavac, K. & Grier, D. G. Microoptomechanical pumps assembled and driven by holographic optical vortex arrays. *Opt. Express* **12**, 1144 (2004).
25. Ward, A. D., Berry, M. G., Mellor, C. D., Bain, C. D. & Baine, C. D. Optical sculpture: controlled deformation of emulsion droplets with ultralow interfacial tensions using optical tweezers. *Chem. Commun. (Camb)*. **16**, 4515–4517 (2006).
26. Dholakia, K., Reece, P. & Gu, M. Optical micromanipulation. *Chemical Society Reviews* vol. 37 42–55 (2008).
27. Padgett, M. & Bowman, R. Tweezers with a twist. *Nature Photonics* vol. 5 343–348 (2011).
28. Padgett, M. & Di Leonardo, R. Holographic optical tweezers and their relevance to lab on chip devices. *Lab Chip* **11**, 1196–1205 (2011).
29. Knight, J. C., Cheung, G., Jacques, F. & Birks, T. A. Phase-matched excitation of whispering-gallery-mode resonances by a fiber taper. *Opt. Lett.* **22**, 1129 (1997).
30. Barber, P. W., Hill, S. C., Lai, H. M., Leung, P. T. & Young, K. Time-independent perturbation for leaking electromagnetic modes in open system with application to resonances in microdroplets. *Phys. Rev. A* **41**, (1990).

## Figures

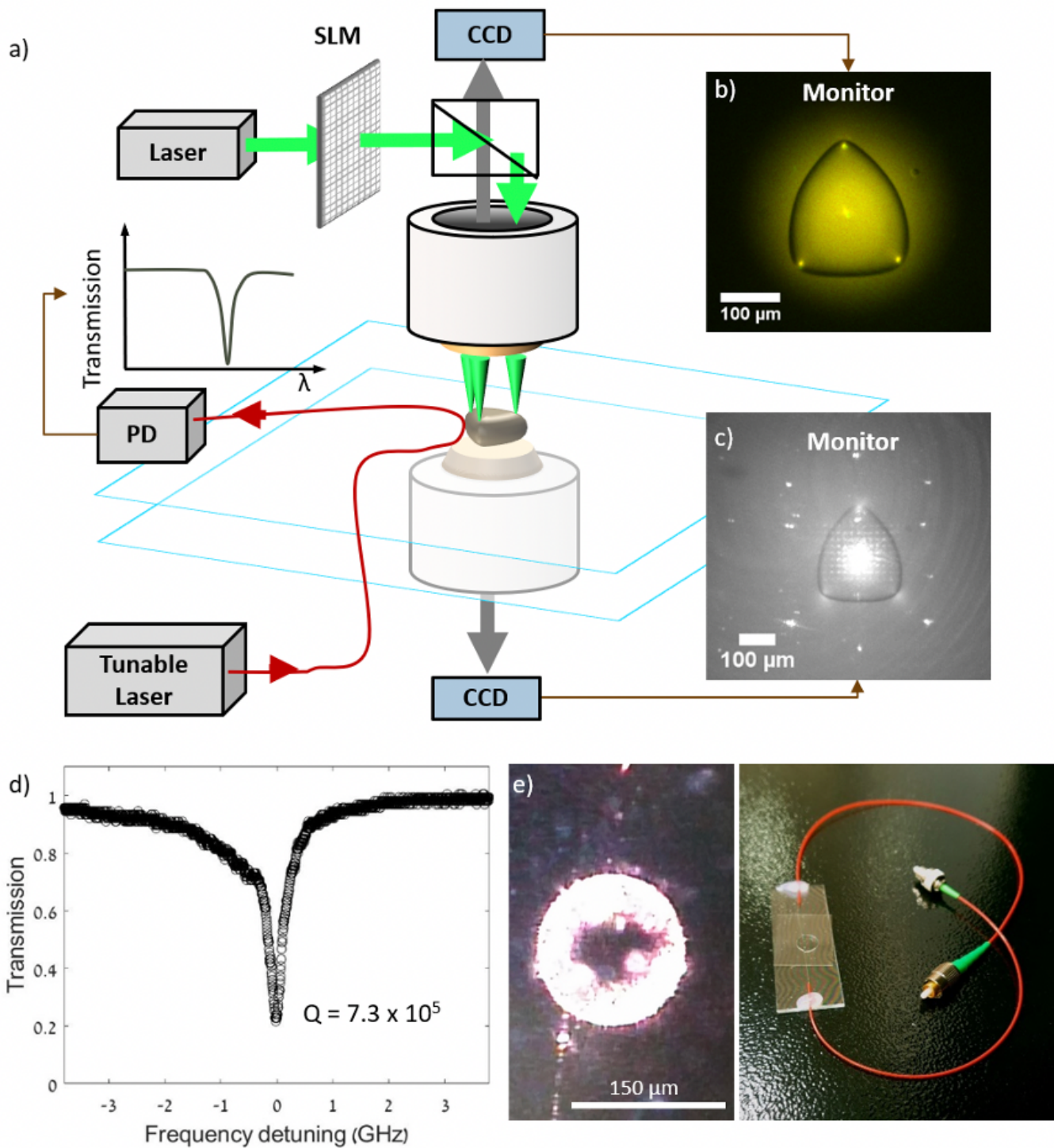


**Figure 1**

Experimental Setup. (a) An n-heptane oil microresonator (golden) in a water chamber (blue) is deformed by a computerized holographic- tweezers (green) into a triangular form while optically accessed as a microcavity using a tunable laser that is coupled to the droplet via a tapered fiber coupler (red). PD: photodetector, SLM: spatial light modulator. (b) Top-view micrograph of a droplet deformed to a triangular shape. The bright dots are the tweezers spots (c) Bottom-view micrograph of the same

deformed droplet. (b) and (c) are micrographs of the real deformed droplet. The bright dots out of the droplets relates to high-order components of the holographic tweezers with insignificant intensity when compared to the first orders. (d) A typical wavelength scan through the solidified resonator resonance reveals transmission dips at resonance, with a quality factor near 730,000. (e) A micrograph of our solidified resonator with light (783 nm) resonating inside.

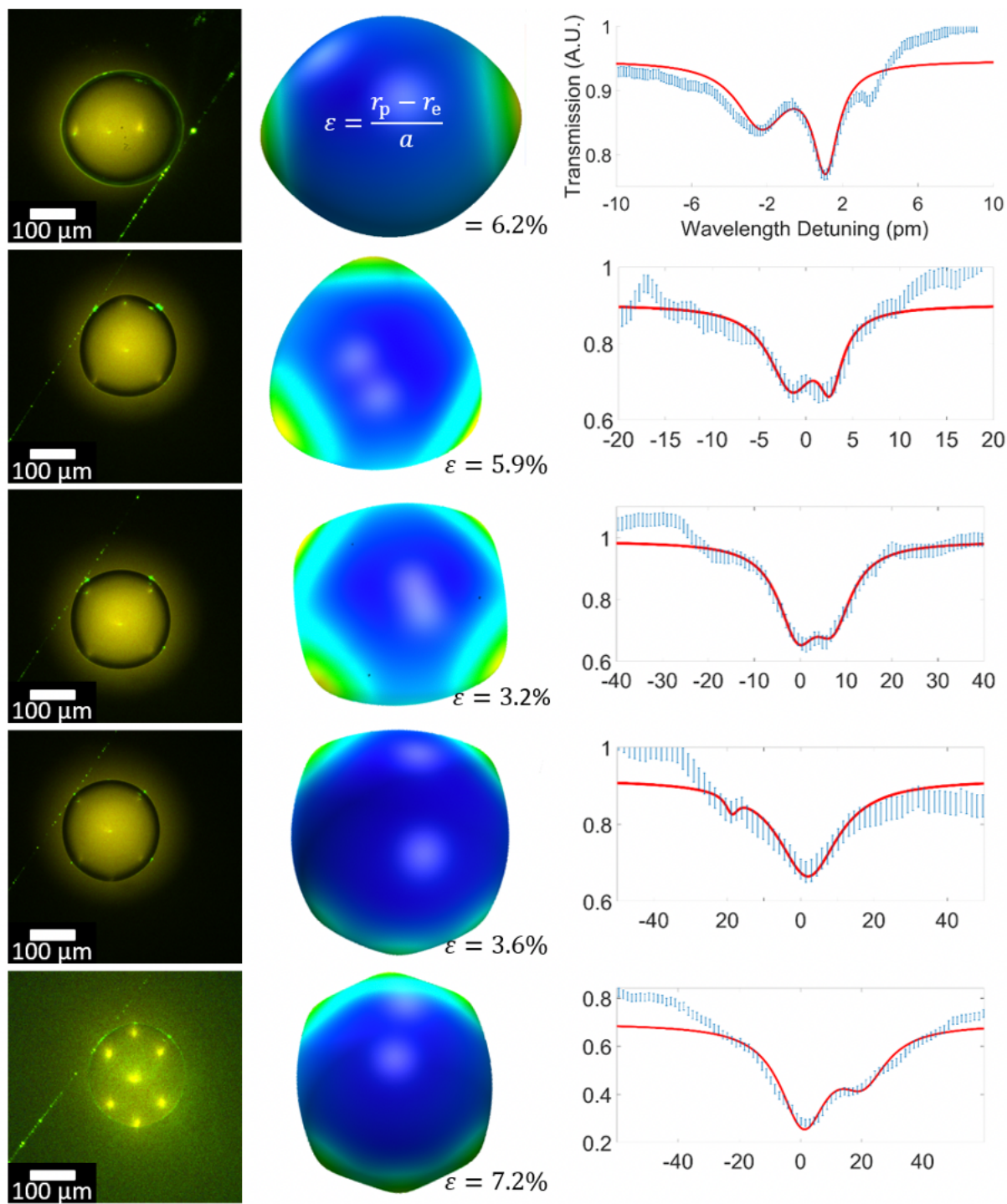


Figure 2

Experimental results: Left: Micrographie of an elliptical, triangular, square, pentagonal, and hexagonal microresonator, deformed with optical tweezers and coupled via tapered fiber. Center: 3D resonator shape image where deformation is exaggerated. Right: The measured transmission, fitted to a two Lorentzian function. Optical wavelength is 780 nm. Error bars represent standard deviation.

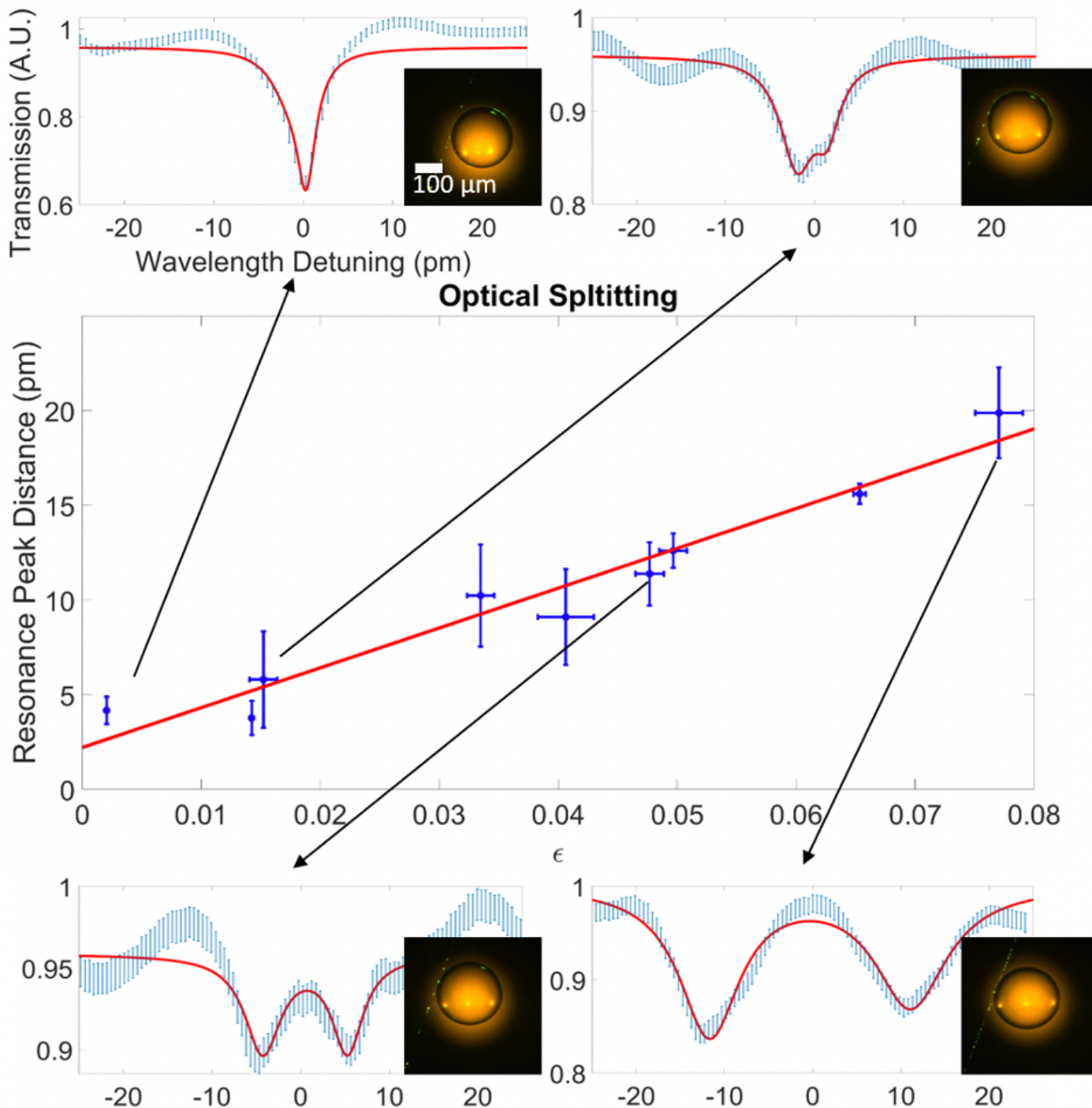
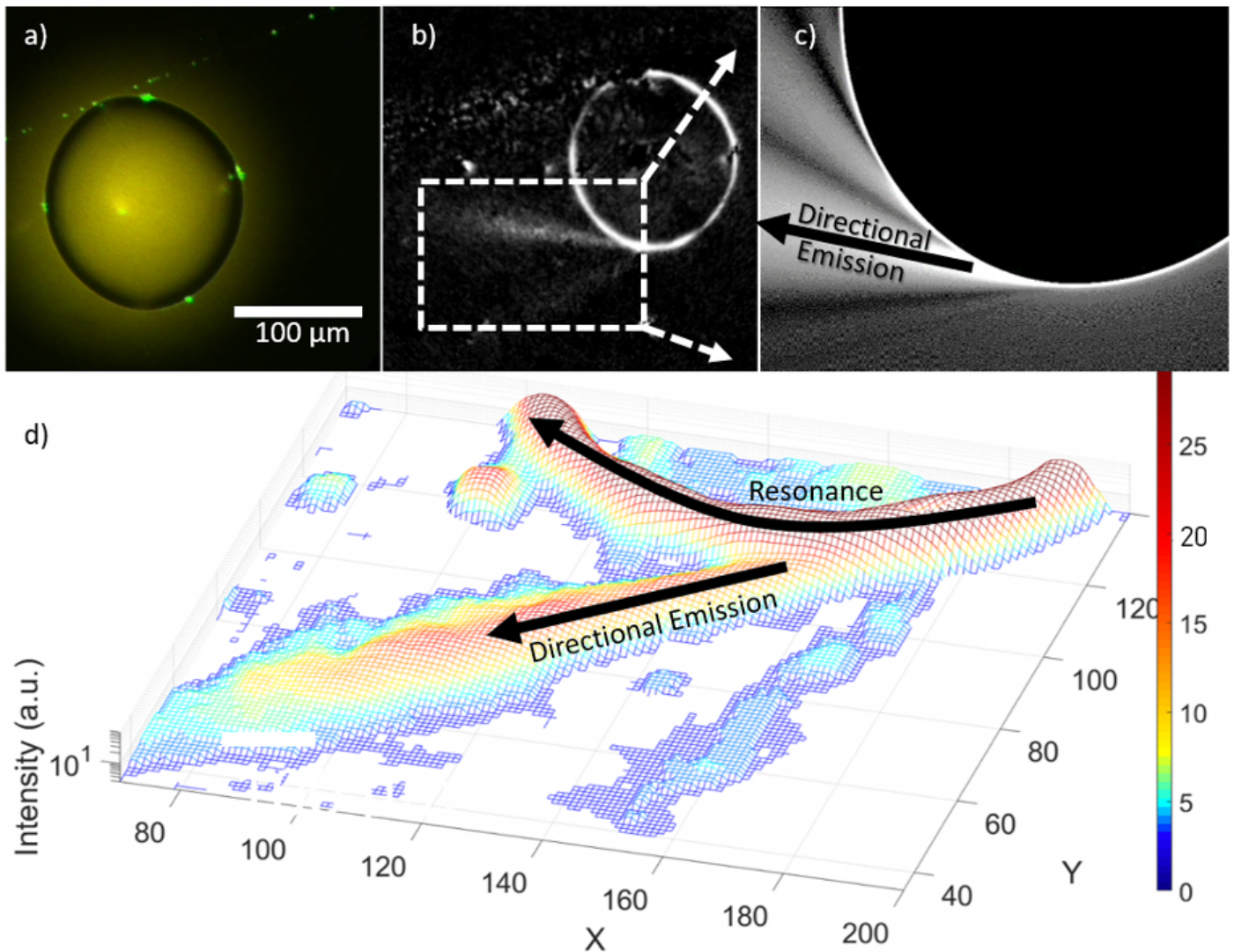


Figure 3

(Central plot) Experimental results, resonance split as a function of deformation Results (blue) are presented with a linear fit (red) with  $r^2 = 0.95$ . Each point in the central plots represents a split anticipated by fitting a two-peak Lorentzian function to the experimentally measured spectral transmission (surrounding plots). Micrographs insets show the deformed droplet that corresponds to the transmission plot. Optical wavelength is 780 nm. Error bars represent standard deviation.



**Figure 4**

Directional emission (a) a micrograph of the arbitrary shaped droplet resonator, taken in visible light where the 4-fold holographic tweezer is seen (green) (b, d) same micrograph taken in the infrared where a deform ring represents the optical resonance and emission is seen from near the region where the curve is sharpest. (c) The results of two-dimensional simulations showing directed emission from an ellipsoidal disk resonator used as a qualitative model for our deformed droplet.

## Supplementary Files

This is a list of supplementary files associated with this preprint. Click to download.

- [NaturePhotonicsMethodSection.docx](#)